*Inorg. Chem.* **2006**, *45*, 7306–7315


# Model Complexes of Cobalt-Substituted Matrix Metalloproteinases: Tools for Inhibitor Design

**Faith E. Jacobsen,[†] Robert M. Breece,[‡] William K. Myers,[‡] David L. Tierney,*[,‡] and Seth M. Cohen*[,†]**

*Department of Chemistry and Biochemistry, University of California, San Diego, La Jolla, California 92093-0358, and Department of Chemistry, University of New Mexico, Albuquerque, New Mexico 87131*

Received May 23, 2006

The tetrahedral cobalt(II) complex [(Tp$^{Ph,Me}$)CoCl] (Tp$^{Ph,Me}$ = hydrotris(3,5-phenylmethylpyrazolyl)borate) was combined with several hydroxypyridinone, hydroxypyridinethione, pyrone, and thiopyrone ligands to form the corresponding [(Tp$^{Ph,Me}$)Co(**L**)] complexes. X-ray crystal structures of these complexes were obtained to determine the mode of binding for each ligand **L**. The structures show that the [(Tp$^{Ph,Me}$)Co(**L**)] complexes are pentacoordinate complexes, with a general tendency toward square pyramidal geometry. The electronic, EPR, and paramagnetic NMR spectroscopy of the [(Tp$^{Ph,Me}$)Co(**L**)] complexes have been examined. The frozen-solution EPR spectra are indicative of pentacoordination in frozen solution, while the NMR indicates some dynamics in ligand binding. The findings presented here suggest that [(Tp$^{Ph,Me}$)Co(**L**)] complexes can be used as spectroscopic references for investigating the mode of inhibitor binding in metalloproteinases of medicinal interest. Potential limitations when using cobalt(II) model complexes are also discussed.

## Introduction

The technique of isomorphous substitution, sometimes referred to as isomorphous replacement, has served to improve the understanding of metalloprotein active sites by replacing spectroscopically silent metals with ions that possess electronic or magnetic properties that can be probed.[1,2] Among the most common and successful replacements is use of the open-shell $d^7$ cobalt(II) to replace the $d^{10}$ closed-shell zinc(II) ion as the metal cofactor in a variety of metalloproteins.[3] The electronic absorption spectra of cobalt(II) complexes have been used to study zinc(II) metalloproteins ranging from zinc-finger transcription factors to hydrolytic enzymes such as carbonic anhydrase.[4−6]

Several studies have prepared and characterized model complexes of zinc(II) and cobalt(II) in order to compare, contrast, and ultimately validate the isomorphous substitution of cobalt(II) frequently applied to zinc metalloproteins.[7,8] A number of these studies have utilized tris(pyrazolyl)borate ligands[9] to model zinc- and cobalt-substituted active sites[10] for carbonic anhydrase[11] and members of the vicinal oxygen chelate (VOC) superfamily of enzymes.[12] Another group of zinc metalloproteins that have been successfully modeled by tris(pyrazolyl)borate ligands are the family of matrix metalloproteinases (MMPs).[13−17] MMPs are calcium- and zinc-dependent hydrolytic metalloenzymes involved in the breakdown of connective tissues (e.g., collagen).[18] Misregulation or overexpression of MMPs is associated with illnesses of

* To whom correspondence should be addressed. Phone: (505) 277-2505 (D.L.T.); (858) 822-5596 (S.M.C). Fax (505) 277-2609 (D.L.T.); (858) 822-5598 (S.M.C.). E-mail: dtierney@unm.edu (D.L.T.); scohen@ucsd.edu (S.M.C.).

[†] University of California.

[‡] University of New Mexico.

(1) Lippard, S. J.; Berg, J. M. *Principles of Bioinorganic Chemistry*; University Science Books: Mill Valley, CA, 1994.
(2) Que, L. J. *Physical Methods in Bioinorganic Chemistry*; University Science Books: Sausalito, CA, 2000.
(3) Maret, W.; Vallee, B. L. *Methods Enzymol.* **1993**, *226*, 52−71.
(4) Bertini, I.; Luchinat, C. *Acc. Chem. Res.* **1983**, *16*, 272−279.
(5) Benelli, C.; Bertini, I.; Di Vaira, M.; Mani, F. *Inorg. Chem.* **1984**, *23*, 1422−1425.
(6) Lachenmann, M. J.; Ladbury, J. E.; Dong, J.; Huang, K.; Carey, P.; Weiss, M. A. *Biochemistry* **2004**, *43*, 13910−13925.
(7) Han, R.; Parkin, G. *J. Am. Chem. Soc.* **1991**, *113*, 9707−9708.
(8) Kremer-Aach, A.; Kläui, W.; Bell, R.; Strerath, A.; Wunderlich, H.; Mootz, D. *Inorg. Chem.* **1997**, *36*, 1552−1563.
(9) Trofimenko, S. *Chem. Rev.* **1993**, *93*, 943−980.
(10) Parkin, G. *Chem. Commun.* **2000**, 1971−1985.
(11) Bergquist, C.; Fillebeen, T.; Morlok, M. M.; Parkin, G. *J. Am. Chem. Soc.* **2003**, *125*, 6189−6199.
(12) Hammes, B. S.; Leo, X.; Chohan, B. S.; Carrano, M. W.; Carrano, C. J. *J. Chem. Soc., Dalton Trans.* **2002**, 3374−3380.
(13) Ruf, M.; Weis, K.; Brasack, I.; Vahrenkamp, H. *Inorg. Chim. Acta* **1996**, *250*, 271−281.
(14) Puerta, D. T.; Cohen, S. M. *Inorg. Chem.* **2002**, *41*, 5075−5082.
(15) Puerta, D. T.; Cohen, S. M. *Inorg. Chim. Acta* **2002**, *337*, 459−462.
(16) Puerta, D. T.; Cohen, S. M. *Inorg. Chem.* **2003**, *42*, 3423−3430.
(17) Jacobsen, F. E.; Cohen, S. M. *Inorg. Chem.* **2004**, *43*, 3038−3047.



10.1021/ic060901u CCC: $33.50 
Published on Web 08/10/2006

**Chart 1.** Compounds Examined in This Study as Chelators of the MMP Active Site Zinc(II) Ion

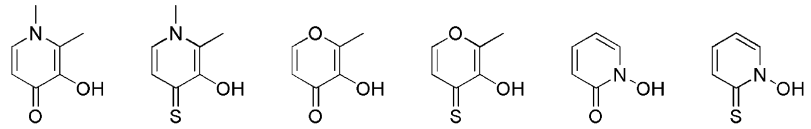


tissue destruction including rheumatoid arthritis, cancer, and heart disease.[19,20] The role of MMPs in human disease has prompted the design of MMP inhibitors (MMPi) that directly bind the MMP active site through a putative zinc-binding group (ZBG).[19] The ZBG is simply a strong metal chelator that binds the zinc(II) ion and thereby suppresses hydrolytic activity. The catalytic zinc ion is bound in the MMP active site by a tris(histidine) metal-binding motif,[21] which has made zinc(II) tris(pyrazolyl)borate complexes suitable models for elucidating the metal−ligand interactions that are important for MMP inhibition.

Recently, we have identified a series of chelators[22] that have an improved ability to inhibit MMPs relative to the more commonly used ZBGs, namely hydroxamic acids.[19,23,24] We have determined the mode of binding for these chelators by using zinc(II) tris(pyrazolyl)borate complexes and have suggested that this mode of binding reflects the coordination geometry at the active site when MMPs are inhibited by these compounds;[16,22] however, these studies do not provide concrete evidence for the mode of coordination of these compounds to the MMP active site. One possible means of correlating model complex structures with the structure inside the MMP active site is by use of model compounds and proteins substituted with cobalt(II). If the zinc(II) and cobalt(II) model complexes are similar, then it is possible to compare electronic, electron paramagnetic resonance (EPR), and NMR spectroscopy of the cobalt complexes with the cobalt-substituted protein to confirm the mode of binding for different ZBGs. Cobalt-substituted MMPs have been prepared for biophysical characterization of the protein active site,[25] as well as for augmenting MMPi design by NMR-based methods.[26] Cobalt(II)-substituted forms of MMPs and the angiotensin converting enzyme (ACE) have both demonstrated distinct changes in the electronic spectra upon the binding of inhibitors.[25−27] EPR has also been a valuable tool for determining active site coordination in cobalt(II) substituted proteins, as well as ligand environment, for the zinc(II) enzymes carboxypeptidase-A and metallo-$\beta$-lactamase.[28,29] Model complexes of the MMP active sites should also reveal similar insight into the binding of these ligands.

Herein, we describe the synthesis, structure, electronic absorption, EPR, and NMR spectroscopy of several tris(pyrazolyl)borate complexes of the general composition [($Tp^{Ph,Me}$)Co(**L**)] ($Tp^{Ph,Me}$ = hydrotris(3,5-phenylmethylpyrazolyl)borate) where **L** is representative of the ZBG (the metal-binding group that would be employed in an MMPi, Chart 1). The $Tp^{Ph,Me}$ ligand was selected on the basis of the intermediate steric requirements of this ligand which permits formation of metal complexes with coordination numbers of 4, 5, and 6.[8] These studies show that the cobalt(II) complexes all have the same coordination number as their zinc(II) analogues and in some cases are isostructural. A tendency for some of the cobalt(II) complexes to be square pyramidal, as opposed to their trigonal bipyramidal zinc(II) counterparts, is observed. While the limitations of these models must be considered, the overall advantage of using these model systems is exemplified in their spectroscopic characterization. Ligand binding dynamics, often inaccessible for metalloproteins due to the limited temperature range available, are easily demonstrated for these systems in organic solvents.

## Experimental Section

**General.** Unless otherwise noted, starting materials were obtained from commercial suppliers (Aldrich) and used without further purification. [($Tp^{Ph,Me}$)Co(Cl)] was prepared according to literature methods.[30] Elemental analysis was performed by NuMega Laboratories, San Diego, California. UV−visible spectra were recorded in $CH_2Cl_2$ using a Perkin-Elmer Lambda 25 spectrophotometer. Absorbance maxima are given as $\lambda_{max}$/nm ($\epsilon$/$M^{-1}$ $cm^{-1}$). Infrared spectra were collected on a Nicolet AVATAR 320 FT-IR instrument at the Department of Chemistry and Biochemistry, University of California, San Diego.

**[($Tp^{Ph,Me}$)Co(3,4-HOPO)].** To a solution of [($Tp^{Ph,Me}$)CoCl] (50 mg, 0.09 mmol) dissolved in 10 mL $CH_2Cl_2$ was added 2−3 drops of triethylamine. To this solution was added 1 equiv of 3,4-HOPO (12 mg, 0.09 mmol) dissolved in 10 mL of $CH_3OH$, resulting in a pink-colored solution. The mixture was stirred at room temperature overnight under a nitrogen atmosphere. After stirring, the solution was evaporated to dryness on a rotary evaporator to give a red solid. The solid was dissolved in a minimum amount of benzene (∼1 mL), filtered to remove any insoluble material, and the filtrate

(18) Massova, I.; Kotra, L. P.; Fridman, R.; Mobashery, S. *FASEB J.* **1998**, *12*, 1075−1095.
(19) Whittaker, M.; Floyd, C. D.; Brown, P.; Gearing, A. J. H. *Chem. Rev.* **1999**, *99*, 2735−2776.
(20) Coussens, L. M.; Fingleton, B.; Matrisian, L. M. *Science* **2002**, *295*, 2387−2392.
(21) Babine, R. E.; Bender, S. L. *Chem. Rev.* **1997**, *97*, 1359−1472.
(22) Puerta, D. T.; Lewis, J. A.; Cohen, S. M. *J. Am. Chem. Soc.* **2004**, *126*, 8388−8389.
(23) Puerta, D. T.; Cohen, S. M., *Curr. Top. Med. Chem.* **2004**, *4*, 1551−1573.
(24) Fisher, J. F.; Mobashery, S. *Cancer Metastasis Rev.* **2006**, *25*, 115−136.
(25) Salowe, S. P.; Marcy, A. I.; Cuca, G. C.; Smith, C. K.; Kopka, I. E.; Hagmann, W. K.; Hermes, J. D. *Biochemistry* **1992**, *31*, 4535−4540.
(26) Bertini, I.; Fragai, M.; Lee, Y.-M.; Luchinat, C. Terni, B. *Angew. Chem., Int. Ed.* **2004**, *43*, 2254−2256.
(27) Bicknell, R.; Holmquist, B.; Lee, F. S.; Martin, M. T.; Riordan, J. F. *Biochemistry* **1987**, *26*, 7291−7297.
(28) Crawford, P. A.; Yang, K.-W.; Sharma, N.; Bennett, B.; Crowder, M. W. *Biochemistry* **2005**, *44*, 5168−5176.
(29) Martinelli, R. A.; Hanson, G. R.; Thompson, J. S.; Holmquist, B.; Pilbrow, J. R.; Auld, D. S.; Vallee, B. L. *Biochemistry* **1989**, *28*, 2251−2258.
(30) Uehara, K.; Hikichi, S.; Akita, M. *J. Chem. Soc., Dalton Trans.* **2002**, 3529−3538.

was recrystallized to give orange blocks by diffusion of the solution with pentane. Yield: 98%. UV−vis ($CH_2Cl_2$): 316 (23649), 445 (379), 555 (89). IR (film from $CH_2Cl_2$): $\nu$ 1064, 1088, 1359, 1549, 2532 (B−H), 3429 $cm^{-1}$. Anal. Calcd for $C_{37}H_{36}N_7O_2BCo$: C, 65.31; H, 5.33; N, 15.03. Found C, 65.70; H, 4.93; N, 14.67.

**[(Tp$^{Ph,Me}$)Co(3,4-HOPTO)].** The same procedure was used as in the synthesis of [(Tp$^{Ph,Me}$)Co(3,4-HOPO)]. The product was a reddish-brown solid. Dark red-brown blocks were grown out of a solution of the complex in benzene diffused with pentane. Yield: 20%. UV−vis ($CH_2Cl_2$): 368 (10996), 505 (273). IR (film from $CH_2Cl_2$): $\nu$ 1066, 1192, 1460, 1547, 1644, 2534 (B−H), 2989, 3061, 3421 $cm^{-1}$. Anal. Calcd for $C_{37}H_{36}N_7OSBCo\cdot 1/4C_6H_6$: C, 64.58; H, 5.28; N, 13.69. Found C, 64.73; H, 5.22; N, 13.84.

**[(Tp$^{Ph,Me}$)Co(maltolato)].** The same procedure was used as in the synthesis of [(Tp$^{Ph,Me}$)Co(3,4-HOPO)]. The product was a red solid. Red blocks were grown out of a solution of the complex in benzene diffused with pentane. Yield: 98%. UV−vis ($CH_2Cl_2$): 324 (7686), 457 (70), 534 (59), 562 (65). IR (film from $CH_2Cl_2$): $\nu$ 687, 768, 1075, 1184, 1584, 2528 (B−H), 3056, 3421 $cm^{-1}$. Anal. Calcd for $C_{36}H_{33}N_6O_3BCo$: C, 64.78; H, 4.98; N, 12.59. Found C, 65.04; H, 4.65; N, 12.89.

**[(Tp$^{Ph,Me}$)Co(thiomaltolato)].** The same procedure was used as in the synthesis of [(Tp$^{Ph,Me}$)Co(3,4-HOPO)]. The product was a an orange-red solid. Dark red-brown blocks were grown out of a solution of the complex in benzene diffused with pentane. Yield: 88%. UV−vis ($CH_2Cl_2$): 309 (12529), 391 (14366), 587 (199), 727 (52). IR (film from $CH_2Cl_2$): $\nu$ 669, 761, 1064, 1180, 1409, 1576, 2535 (B−H), 2924, 3060, 3405 $cm^{-1}$. Anal. Calcd for $C_{36}H_{33}BCoN_6O_2S$: C, 63.26; H, 4.87; N, 12.30. Found C, 63.66; H, 4.81; N, 11.92.

**[(Tp$^{Ph,Me}$)Co(1,2-HOPO)].** The same procedure was used as in the synthesis of [(Tp$^{Ph,Me}$)Co(3,4-HOPO)]. The product was a pink solid. Pink blocks were grown out of a solution of the complex in benzene diffused with pentane. Yield: 92%. UV−vis ($CH_2Cl_2$): 310 (4651), 461 (51), 524 (44), 551 (40), 699 (14). IR (film from $CH_2Cl_2$): $\nu$ 1169, 1471, 1530, 1616, 2497 (B−H), 2955, 2979, 3394 $cm^{-1}$. Anal. Calcd for $C_{34}H_{32}N_7O_2BCo$: C, 64.43; H, 4.94; N, 15.03. Found C, 64.73; H, 4.76; N, 15.43.

**[(Tp$^{Ph,Me}$)Co(1,2-HOPTO)].** The same procedure was used as in the synthesis of [(Tp$^{Ph,Me}$)Co(3,4-HOPO)]. The product was a dark reddish-brown solid. Dark red-orange blocks were grown out of a solution of the complex in benzene diffused with pentane. Yield: 87%. UV−vis ($CH_2Cl_2$): 320 (9014), 382 (1665), 483 (136). IR (film from $CH_2Cl_2$): $\nu$ 697, 764, 1066, 1192, 1459, 1544, 2498 (B−H), 2979, 3058 $cm^{-1}$. Anal. Calcd for $C_{34}H_{32}N_7OSBCo\cdot 1.5H_2O$: C, 60.44; H, 5.07; N, 14.10. Found C, 60.29; H, 4.98; N, 14.08.

**[(Tp$^{Ph,Me}$)Co(pz$^{Ph,Me}$)Cl].** This compound was obtained as a decomposition product from complexation reactions that did not include triethylamine (vide infra). Magenta prisms were grown by recrystallization from a benzene solution of the complex diffused with pentane. UV−vis ($CH_2Cl_2$): 312 (5564), 345 (5728), 383 (1101), 568 (37). IR (film from $CH_2Cl_2$): $\nu$ 1076, 1177, 1429, 1542, 2528 (B−H), 2684, 2994, 3052 $cm^{-1}$. Anal. Calcd for $C_{40}H_{37}N_8BClCo$: C, 65.37; H, 5.07; N, 15.25. Found C, 65.15; H, 5.41; N, 15.56.

**X-ray Crystallographic Analysis.** Data were collected on a Bruker AXS area detector diffractometer. Crystals were mounted on quartz capillaries by using Paratone oil and were cooled in a nitrogen stream (Kryo-flex controlled) on the diffractometer (−173 °C). Peak integrations were performed with the Siemens SAINT software package. Absorption corrections were applied using the program SADABS. Space group determinations were performed by the program XPREP. The structures were solved by direct or Patterson methods and refined with the SHELXTL software package.[31] Unless noted otherwise, all hydrogen atoms, except for the boron hydrogen atoms, were fixed at calculated positions with isotropic thermal parameters; all non-hydrogen atoms were refined anisotropically. Co-crystallized solvent was found in three structures. In [(Tp$^{Ph,Me}$)Co(pz$^{Ph,Me}$)Cl], the asymmetric unit contains one molecule of benzene. In [(Tp$^{Ph,Me}$)Co(thiomaltolato)], the asymmetric unit contained several disorder solvent molecules. Squeeze[32] was used to treat what appeared to be two molecules of pentane and two molecules of benzene (Expected $e^-$ count/cell: 168. Found: 164). In [(Tp$^{Ph,Me}$)Co(3,4-HOPTO)], the structure contained four independent molecules in the asymmetric unit, as well as heavily disorder solvent. Squeeze[32] was used to treat what appeared to be 1.5 molecules of pentane and two molecules of benzene (Expected $e^-$ count/cell: 144. Found: 147). X-ray crystallographic data are available from the Cambridge Crystallographic Data Centre (http://www.ccdc.cam.ac.uk). Refer to CCDC reference numbers 244909. 244911, 244912, 244913, 608004, 608005, and 608006.

**EPR Spectroscopy.** Frozen-solution X-band EPR spectra were recorded on a Bruker EMX EPR spectrometer, with temperature maintained by an Oxford ESR-900 liquid He cryostat. All samples were 20 mM in 50:50 (v/v) toluene/dichloromethane glasses; all samples were thoroughly degassed by multiple freeze−pump−thaw cycles prior to data collection. The spectra presented herein were recorded using the following conditions: $T = 3.8$ K; $\nu_{MW} = 9.4$ GHz (2 mW); 5 G field modulation (100 kHz); receiver gain = 5000; time constant = 82 ms. EPR spectra were simulated with full matrix diagonalization, using the program XSOPHE (Bruker Biospin), employing a *g*-strain model to match the apparent line widths.[33] To arrive at the final simulations, the magnitude of *D* was reduced to the minimum value necessary to reproduce the spectral features, and therefore, the value of *D* reported in Table 3 should be taken as a lower limit of the axial zero-field splitting (zfs) for these systems. In general, the sensitivity of the simulation to the magnitude of *D* was proportional to the value of *D* used—those requiring a smaller value of *D* were more sensitive to changes in this value.

**NMR Spectroscopy.** NMR spectra were recorded on a Bruker ASX (300 MHz) spectrometer. Temperature control was accomplished with a liquid-$N_2$ evaporator and the heater/thermocouple provided with the instrument. Chemical shifts were referenced to the $^1H$ resonances of the solvent, toluene, which also served as an internal standard for temperature calibration. All NMR samples were 20 mM in toluene-$d_8$ (use of 50:50 toluene/dichloromethane as solvent had no effect on the spectra), and all were subjected to several freeze−pump−thaw cycles prior to data collection. The spectra presented here are the average of 1024 scans that consist of 8k data points over a spectral window of 150 kHz (500 ppm), using a 3 $\mu$s excitation pulse. The FID was smoothed by exponential multiplication, which incorporated an additional line width of 5 Hz.

## Results and Discussion

The goal of this investigation was two-fold: the first goal was to compare the coordination geometry of [(Tp$^{Ph,Me}$)Co(**L**)] complexes with those of the corresponding zinc(II)

(31) Sheldrick, G. M. *SHELXTL ver. 5.1 Software Reference Manual*; Bruker AXS: Madison, WI, 1997.
(32) Spek, A. *Platon Library*.
(33) Griffin, M.; Muys, A.; Noble, C.; Wang, D.; Eldershaw, C.; Gates, K. E.; Burrage, K.; Hanson, G. R. *Mol. Phys. Rep.* **1999**, *26*, 60−84.

**Table 1.** X-ray Structure Data for All [(Tp$^{Ph,Me}$)Co(**L**)] Complexes and [(Tp$^{Ph,Me}$)Co(pz$^{Ph,Me}$)Cl]

| | [(Tp$^{Ph,Me}$)Co(pz$^{Ph,Me}$)Cl] | [(Tp$^{Ph,Me}$)Co(maltolato)] | [(Tp$^{Ph,Me}$)Co(thiomaltolato)] | [(Tp$^{Ph,Me}$)Co(3,4-HOPO)] |
|---|---|---|---|---|
| empirical formula | $C_{46}H_{43}BClN_8Co$ | $C_{36}H_{33}BN_6O_3Co$ | $C_{36}H_{33}BN_6O_2SCo$ | $C_{37}H_{36}BN_7O_2Co$ |
| cryst syst | monoclinic | monoclinic | trigonal | monoclinic |
| space group | $P2_1/c$ | $Pn_1/n$ | $R\bar{3}$ | $P2_1/n$ |
| *a* | 15.7335(14) Å | 14.8317(15) Å | 25.1695(6) Å | 12.2416(6) Å |
| *b* | 11.8704(11) Å | 13.1243(14) Å | 25.1695(6) Å | 11.1270(5) Å |
| *c* | 21.967(2) Å | 17.0806(18) Å | 29.1776(13) Å | 24.7469(12) Å |
| α | 90° | 90° | 90° | 90° |
| *β* | 101.359(2)° | 103.534(2)° | 90° | 101.086(1)° |
| *γ* | 90° | 90° | 120° | 90° |
| *V*, *Z* | 4022.3(6) Å$^3$, 4 | 3232.5(6) Å$^3$, 4 | 16007.7(9) Å$^3$, 18 | 3307.9(3) Å$^3$, 4 |
| cryst size | 0.41 × 0.22 × 0.12 mm$^3$ | 0.25 × 0.15 × 0.10 mm$^3$ | 0.35 × 0.30 × 0.20 mm$^3$ | 0.30 × 0.15 × 0.15 mm$^3$ |
| *T* (K) | 100(2) | 213(2) | 100(2) | 213(2) |
| reflns collected | 34 277 | 22 150 | 30 053 | 23 188 |
| independent reflns | 9625 [*R*(int) = 0.0419] | 7275 [*R*(int) = 0.0481] | 8121 [*R*(int) = 0.0224] | 7458 [*R*(int) = 0.0311] |
| data/restraint/params | 9625/0/522 | 7275/0/432 | 8127/0/428 | 7458/0/432 |
| GOF on $F^2$ | 1.074 | 1.095 | 1.072 | 0.999 |
| final *R* indices $I > 2\sigma(I)$[a] | R1 = 0.0493 wR2 = 0.1218 | R1 = 0.0531 wR2 = 0.1261 | R1 = 0.0328 wR2 = 0.0942 | R1 = 0.0456 wR2 = 0.1184 |
| *R* indices (all data)[a] | R1 = 0.0582 wR2 = 0.1267 | R1 = 0.0657 wR2 = 0.1318 | R1 = 0.0367 wR2 = 0.0965 | R1 = 0.0558 wR2 = 0.1254 |

| | [(Tp$^{Ph,Me}$)Co(3,4-HOPTO)] | [(Tp$^{Ph,Me}$)Co(1,2-HOPO)] | [(Tp$^{Ph,Me}$)Co(1,2-HOPTO)] |
|---|---|---|---|
| empirical formula | $C_{37}H_{36}BN_7OSCo$ | $C_{35}H_{32}BN_7O_2Co$ | $C_{35}H_{32}BN_7OSCo$ |
| cryst syst | monoclinic | monoclinic | monoclinic |
| space group | *Pn* | $P2_1/c$ | $P2_1/c$ |
| *a* | 11.9410(9) Å | 15.406(4) Å | 14.967(2) Å |
| *b* | 18.3271(14) Å | 12.774(3) Å | 12.780(2) Å |
| *c* | 33.683(3) Å | 18.238(5) Å | 17.131(3) Å |
| α | 90° | 90° | 90° |
| *β* | 97.3270(10)° | 107.138(4)° | 105.238(2)° |
| *γ* | 90° | 90° | 90° |
| *V*, *Z* | 7311.1(10) Å$^3$, 8 | 3429.9(16) Å$^3$, 4 | 3161.8(9) Å$^3$, 4 |
| cryst size | 0.20 × 0.10 × 0.05 mm$^3$ | 0.30 × 0.25 × 0.20 mm$^3$ | 0.35 × 0.30 × 0.25 mm$^3$ |
| *T* (K) | 100(2) | 100(2) | 100(2) |
| reflns collected | 61 742 | 24 256 | 26 503 |
| independent reflns | 31 668 [*R*(int) = 0.0669] | 7057 [*R*(int) = 0.0363] | 7160 [*R*(int) = 0.0361] |
| data/restraint/params | 31 668/2/1765 | 7057/0/422 | 7160/0/422 |
| GOF on $F^2$ | 0.940 | 1.183 | 1.024 |
| final *R* indices $I > 2\sigma(I)$[a] | R1 = 0.0573 wR2 = 0.1096 | R1 = 0.0437 wR2 = 0.1245 | R1 = 0.0354 wR2 = 0.0840 |
| *R* indices (all data)[a] | R1 = 0.0879 wR2 = 0.1199 | R1 = 0.0518 wR2 = 0.1389 | R1 = 0.0470 wR2 = 0.0896 |

[a] $R1 = \sum||F_o| - |F_c||/\sum|F_o|$, $wR2 = \{\sum[w(F_o^2 - F_c^2)^2]/\sum[wF_o^4]\}^{1/2}$.

complexes. The second goal was to thoroughly examine the spectroscopy of the [(Tp$^{Ph,Me}$)Co(**L**)] complexes to better understand and benchmark the spectroscopic parameters for relevant cobalt(II) complexes with known coordination environments. The ligands selected were chosen on the basis of their potential use in MMPi (Chart 1).[16,22] The results presented here are designed to determine the limitations and strengths of ligand binding to a cobalt(II) ion in an MMP model complex as compared with analogous zinc(II) complexes prepared from [(Tp$^{Ph,Me}$)ZnOH]. If the structures of these model compounds are sufficiently similar for zinc(II) and cobalt(II), then these complexes could allow for determination of the ligand binding in the native holoprotein, thereby establishing a spectroscopic handle for probing the binding mode of different chelators in cobalt(II)-substituted MMPs. Such spectroscopic standards can be used as a tool for characterizing the metal−ligand interactions of metalloprotein inhibitors.

Although an earlier study reported the synthesis of a [(Tp)CoOH] complex,[11] which was a potential intermediate for the desired heteroleptic complexes, we sought a more convenient method to preparing the complexes of interest.[34]

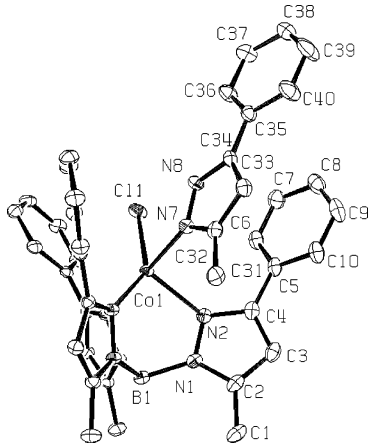


**Figure 1.** Structural diagram of [(Tp$^{Ph,Me}$)Co(pz$^{Ph,Me}$)Cl] with partial atom numbering schemes (ORTEP, 50% probability ellipsoids). Hydrogen atoms have been omitted for clarity.

An investigation that described the preparation of [(Tp)Co(**L**)] compounds via a [(Tp)CoCl] intermediate presented an intriguing route;[30] however, the procedure typically required the preparation of silver(I) salts of the ligand **L** to remove the cobalt-bound halide.[8] Using the latter procedure as a lead, a deep blue solution of [(Tp$^{Ph,Me}$)CoCl] in $CH_2Cl_2$ was mixed with a MeOH solution of the bidentate ligand 3,4-HOPO, resulting in a yellow-green mixture. Upon stirring overnight,

(34) Ruf, M.; Noll, B. C.; Groner, M. D.; Yee, G. T.; Pierpont, C. G. *Inorg. Chem.* **1997**, *36*, 4860−4865.

**Scheme 1.** General Synthesis for [(Tp$^{Ph,Me}$)Co(**L**)] Complexes (**L** = 3,4-HOPO Shown)

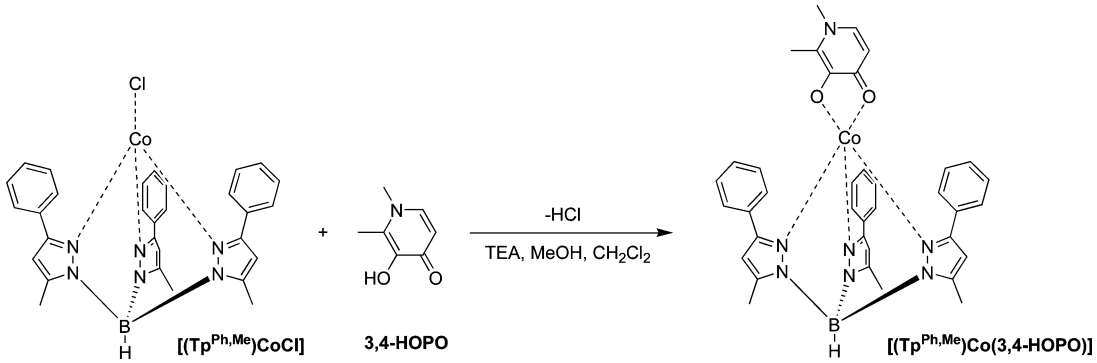


the solution changed to a peach color, and upon removal of solvent, a light green solid was obtained. Recrystallization of this material generated dark magenta crystals that were structurally characterized (Table 1) and found to be the complex [(Tp$^{Ph,Me}$)Co(pz$^{Ph,Me}$)Cl]. The structure shows a distorted trigonal bipyramidal coordination geometry ($\tau$ = 0.58),[35] with the pz$^{Ph,Me}$ and one of the Tp$^{Ph,Me}$ nitrogen donor atoms comprising the axial positions of the coordination sphere (Figure 1). The average Co−N bond length is 2.12 Å, and the Co−Cl bond length is 2.32 Å. Similar decomposition products have been observed in other tris(pyrazolyl)-borate complexes and were attributed to possible metal-promoted hydrolytic chemistry.[12,36−39] In the present case, these findings also suggested that the HCl generated upon complexation of an exogenous ligand such as 3,4-HOPO did not allow the reaction to go to completion and ultimately may have resulted in acid-promoted decomposition of the starting material to generate [(Tp$^{Ph,Me}$)Co(pz$^{Ph,Me}$)Cl]. On the basis of this hypothesis, a simple, efficient synthesis for preparing the desired heteroleptic complexes was developed starting from [(Tp$^{Ph,Me}$)CoCl]. The compounds in Chart 1 were each combined with [(Tp$^{Ph,Me}$)CoCl] in a mixture of $CH_2Cl_2$ and MeOH with excess triethylamine (TEA) to generate the resulting [(Tp$^{Ph,Me}$)Co(**L**)] complexes (Scheme 1). The [(Tp$^{Ph,Me}$)Co(**L**)] complexes were then recrystallized by diffusing pentane into a solution of the cobalt(II) complex in benzene. The TEA is an adequate base for neutralizing the HCl generated in the reaction, and the complexation reactions proceed smoothly and in good yield. The route devised for preparing these [(Tp$^{Ph,Me}$)Co(**L**)] complexes is general and facile, eliminating the requirement for removing the halide with silver(I), and alleviating the necessity for purification by chromatography.[8] The structures of each complex synthesized herein were determined by single-crystal X-ray diffraction. In addition, these complexes have been characterized by elemental analysis, absorbance, IR, paramagnetic NMR, and EPR spectroscopy.

With a general route to [(Tp$^{Ph,Me}$)Co(**L**)] complexes established, several complexes were prepared with ligands that were anticipated to be bidentate chelators based on the corresponding zinc(II) complexes. The ligands in Chart 1 were selected on the basis of their importance as proposed ZBGs for use in MMPi;[16,22] all six compounds are found to be more potent than the common hydroxamic acid ZBG used in most MMPi.[22] The [(Tp$^{Ph,Me}$)Co(**L**)] complexes were prepared as described above and structurally characterized, which revealed that all six ligands shown in Chart 1 bind in a bidentate fashion, forming pentacoordinate cobalt(II) complexes (Figure 2). The crystallographic details of the [(Tp$^{Ph,Me}$)Co(**L**)] complexes are summarized in Table 1. Initial inspection of the [(Tp$^{Ph,Me}$)Co(**L**)] complexes suggests that the coordination of these chelators to cobalt(II) will parallel those in [(Tp$^{Ph,Me}$)Zn(**L**)] compounds.[16]

Although all six complexes show cobalt(II) ions with a coordination number of five (Figure 2), the coordination geometries of the [(Tp$^{Ph,Me}$)Co(**L**)] complexes generally differ from their zinc(II) counterparts (Table 2). The geometry of the cobalt(II) [(Tp$^{Ph,Me}$)Co(**L**)] complexes reported here possess distorted square pyramidal geometries ($\tau$ values of 0.17−0.37), in contrast to the more trigonal bipyramidal structures found for the analogous [(Tp$^{Ph,Me}$)Zn(**L**)] complexes.[16,22] Of the earlier reported zinc(II) complexes, only [(Tp$^{Ph,Me}$)Zn(3,4-HOPO)] has a distorted square pyramidal coordination sphere and is essentially isomorphous to [(Tp$^{Ph,Me}$)Co(3,4-HOPO)].[16] In the cobalt(II) complexes, a pyrazole nitrogen atom occupies the axial position on the coordination sphere. Also, in all cases, the O,S donor ligands form more perfectly square pyramidal structures (i.e., smaller $\tau$ values), while retaining the pyrazole nitrogen as the axial ligand.

From the crystallographic data, it is important to recognize that the information obtained from cobalt(II) model complexes must be utilized with some discretion. While the model complexes are able to predict the correct coordination number, in most cases, a greater tendency toward square pyramidal geometry is observed (relative to the analogous zinc(II) complexes). This trend is expected in the solid state, as there is a slight ligand-field stabilization energy for $d^7$ configurations in the square pyramidal arrangement.[40−45] In

(35) Addison, A. W.; Rao, T. N.; Reedijk, J.; van Rijn, J.; Verschoor, G. C. *J. Chem. Soc., Dalton Trans.* **1984**, 1349−1356.
(36) Siemer, C. J.; Meece, F. A.; Armstrong, W. H.; Eichhorn, D. M. *Polyhedron* **2001**, *20*, 2637−2646.
(37) Sugawara, K.-I.; Hikichi, S.; Akita, M. *J. Chem. Soc., Dalton Trans.* **2002**, 4514−4525.
(38) Kimi-Hunt, E.; Spartalian, K.; DeRusha, M.; Nunn, C. M.; Carrano, C. J. *Inorg. Chem.* **1989**, *28*, 8.
(39) Long, D. P.; Chandrasekaran, A.; Day, R. O.; Bianconi, P. A.; Rheingold, A. L. *Inorg. Chem.* **2000**, *39*, 4476−4487.
(40) Muetterties, E. L.; Schunn, R. A. *Quart. Rev., Chem. Soc.* **1966**, *20*, 245−299.

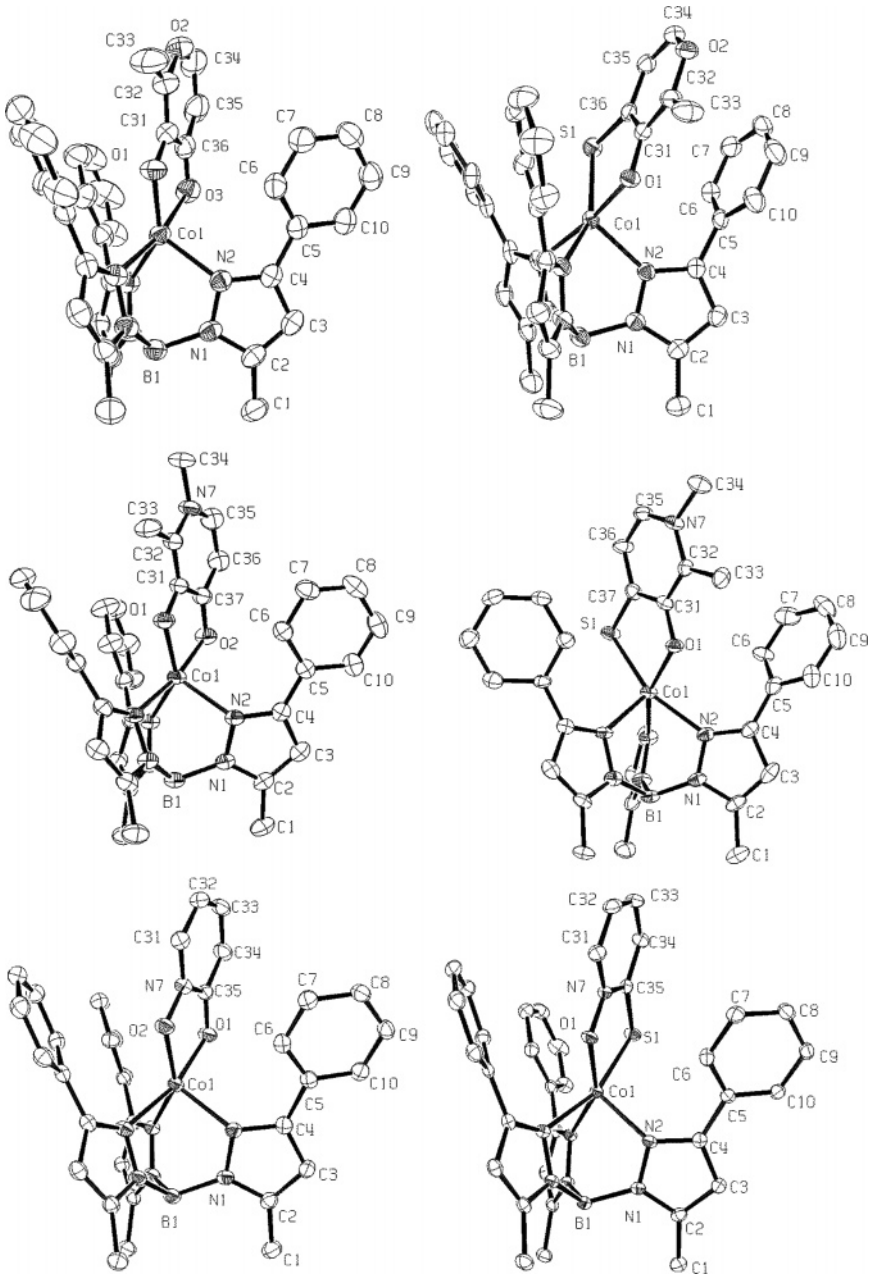


**Figure 2.** Structural diagrams of [(Tp$^{Ph,Me}$)Co(**L**)] complexes with partial atom numbering schemes (ORTEP, 50% probability ellipsoids). Hydrogen atoms, solvent molecules, and one phenyl ring in [(Tp$^{Ph,Me}$)Co(3,4-HOPTO)**]** have been omitted for clarity. For each row (left, right): **L** = maltol, thiomaltol (top); **L** = 3,4-HOPO, 3,4-HOPTO (middle); **L** = 1,2-HOPO, 1,2-HOPTO (bottom).

solution, the energy difference between square pyramidal and trigonal bipyramidal configurations is small, with the two forms rapidly transforming via either a Berry pseudorotation or through dissociation and recombination.[44] In fact, other studies have been able to isolate both geometric isomers in the solid state,[45] further emphasizing the small energy barrier between the two pentacoordinate geometries. It has also been shown that the solid-state electronic spectra of each geometry are similar, making prediction of the geometry solely on the basis of differences in the electronic spectra difficult.[45] It follows that the solution electronic spectra of our model complexes, with an equilibrium between the two geometries, would generate spectra that would reveal the coordination mode of the ligand in cobalt(II)-substituted proteins. Despite any bias toward a square pyramidal geometry, the electronic spectra would still be useful for determining the coordination number of the metal center.

The electronic spectra of all of the cobalt(II) complexes were obtained in $CH_2Cl_2$ solution. Representative spectra are shown in Figure 3; a separate plot highlights the ligand-field transitions of interest. In the ligand-field region, the strongly chelating ligands from Chart 1 show broad, weak

(41) Rossi, A. R.; Hoffmann, R. *Inorg. Chem.* **1975**, *14*, 365−374.
(42) Cotton, F. A.; Wilkinson, G.; Murillo, C. A.; Bochmann, M. *Advanced Inorganic Chemistry*, 6th ed.; Wiley: New York, 1999.
(43) Greenwood, N. N.; Earnshaw, A. *Chemistry of the Elements*; Pergamon: Oxford, 1984.
(44) Huheey, J. E.; Keiter, E. A.; Keiter, R. L. *Inorganic Chemistry*; HarperCollins: New York, 1993.
(45) Stalick, J. K.; Corfield, P. W. R.; Meek, D. W. *Inorg. Chem.* **1973**, *12*, 1668−1675.

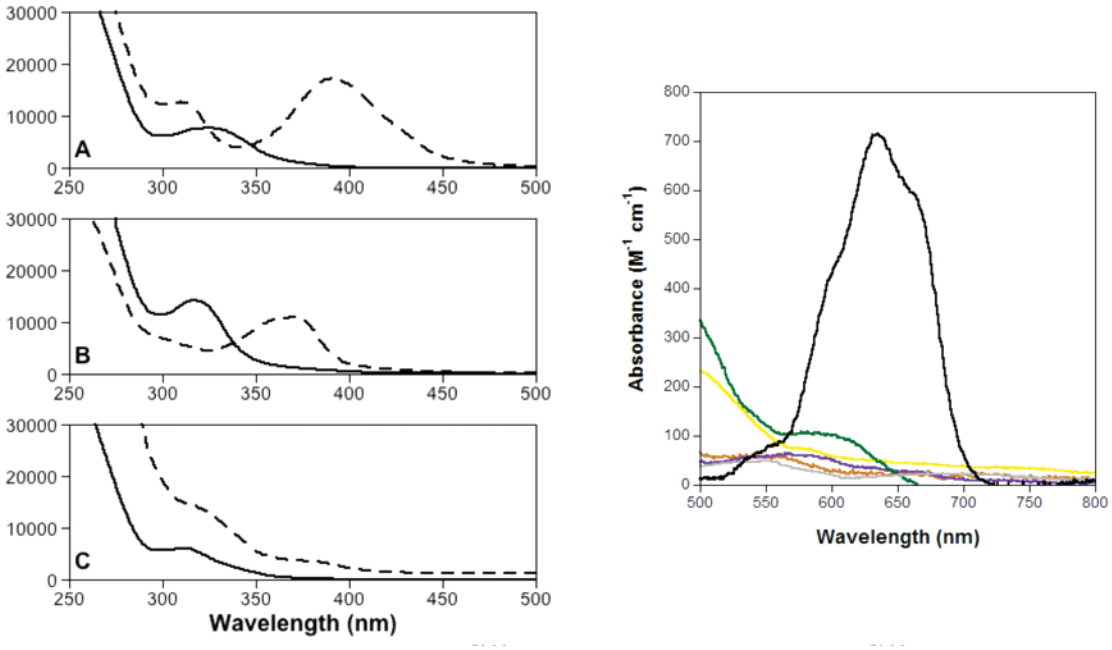


**Figure 3.** Electronic spectra (left) of [(Tp$^{Ph,Me}$)Co(**L**$_{O,O}$)] (solid lines) and [(Tp$^{Ph,Me}$)Co(**L**$_{O,S}$)] (dashed lines) complexes in $CH_2Cl_2$ solution ($y$ axis is $\epsilon$ in $M^{-1}$ cm$^{-1}$). (A) L = maltol, thiomaltol; (B) 3,4-HOPO, 3,4-HOPTO; (C) 1,2-HOPO, 1,2-HOPTO. Ligand-field transitions (right) of [(Tp$^{Ph,Me}$)Co(3,4-HOPO)] (orange), [(Tp$^{Ph,Me}$)Co(3,4-HOPTO)] (yellow), [(Tp$^{Ph,Me}$)Co(maltolato)] (purple), [(Tp$^{Ph,Me}$)Co(thiomaltolato)] (green), [(Tp$^{Ph,Me}$)Co(1,2-HOPO)] (gray), [(Tp$^{Ph,Me}$)Co(1,2-HOPTO)] (blue), and [(Tp$^{Ph,Me}$)Co(Cl)] (black) in $CH_2Cl_2$.

transitions, indicative of a 5-coordinate geometry, while the monodentate chloride in [(Tp$^{Ph,Me}$)Co(Cl)] results in more intense d−d transitions.[46] The electronic spectrum of [(Tp$^{Ph,Me}$)Co(Cl)] demonstrates that the d−d transitions that are typically present for tetracoordinate complexes in solution are clearly absent for the pentacoordinate complexes. Similar d−d transitions have been reported for cobalt(II)-substituted MMP-3 and MMP-13 when complexed to monodentate thiol inhibitors that generate a tetracoordinated metal center in the protein.[25,26] The extinction coefficients observed for the pentacoordinate species are slightly smaller than anticipated, suggesting higher-than-expected symmetry in these complexes.[47]

At higher energies, the cobalt(II) complexes show a variety of intense transitions, depending on the nature of the metal chelator. All of the complexes show a fairly intense transition near 320 nm that most likely arises from oxygen-to-metal charge-transfer. The sulfur-containing derivatives give rise to a second transition between 370 and 400 nm that can be ascribed to sulfur-to-metal charge-transfer. Thiomaltol displays the most intense of these, and this has the effect of blue-shifting the oxygen-to-metal charge-transfer, reflecting an electron-withdrawing effect of the sulfur on the oxygen of thiomaltol. The sulfur-to-metal charge-transfer of 3,4-HOPTO is blue-shifted, relative to thiomaltol, and the oxygen-to-metal charge-transfer is nearly absent for this complex. This may reflect a further blue-shift of the oxygen-to-metal transition or simply diminished intensity. The sulfur-containing *N*-oxide, 1,2-HOPTO, shows the weakest of the sulfur-to-metal transitions and the strongest of the oxygen-to-metal transitions, suggesting more equal charge balance across the donor atoms of this ligand. In general, on the basis of the energies and extinction coefficients, the spectra likely involve a combination of both charge-transfer and ligand-centered transitions. Electronic spectra of the free ligands and their homoleptic complexes with a variety of transition metal ions, including cobalt(II), are consistent with the observed complexity in the spectra.[48,49] The characteristic features found in this region of the electronic spectra will prove useful in confirming active-site binding of these chelators in cobalt(II)-substituted MMPs.

X-band, low-temperature EPR spectra of the cobalt(II) complexes are presented in Figure 4 (black lines). The spectra are consistent with low-to-moderate symmetry, pentacoordinate complexes of high-spin cobalt(II),[29,50−52] with modest variations, dependent on the ancillary ligand. Simulations (gray lines in Figure 4) match the features in the data, although some intensity discrepancies persist. The simulations, summarized in Table 3, indicate that the observed spectra arise from transitions within both the $\pm^1/_2$ and $\pm^3/_2$ doublets, with no apparent transitions between them. In general, the resolved hyperfine structure near $g = 8.6$ and the high-field derivative signal arise from the lower $\pm^3/_2$ doublet. The broad underlying features near $g = 6$ (to the high-field end of the hyperfine pattern), the derivative feature near $g = 4$, and unresolved features near $g = 2$ arise from

(46) Kunz, P. C.; Reib, G. J.; Frank, W.; Kläui, W. *Eur. J. Inorg. Chem.* **2003**, 3945−3951.
(47) Lever, A. B. P. *Inorganic Electronic Spectroscopy*, 2nd ed.; Elsevier: Amsterdam, 1984.
(48) Lewis, J. A.; Puerta, D. T.; Cohen, S. M. *Inorg. Chem.* **2003**, *42*, 7455−7459.
(49) Lewis, J. A.; Tran, B. L.; Puerta, D. T.; Rumberger, E. M.; Hendrickson, D. N.; Cohen, S. M. *Dalton Trans.* **2005**, 2588−2596.
(50) Bencini, A.; Bertini, I.; Canti, G.; Gatteschi, D.; Luchinat, C. *J. Inorg. Biochem.* **1981**, *14*, 81−93.
(51) Li, T. F.; Walker, A. L.; Iwaki, H.; Hasegawa, Y.; Liu, A. M. *J. Am. Chem. Soc.* **2005**, *127*, 12282−12290.
(52) Bertini, I.; Luchinat, C. *Adv. Inorg. Biochem.* **1984**, *6*, 71−111.

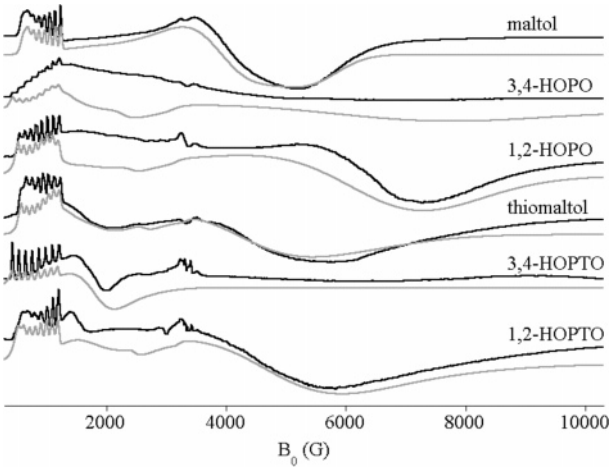


**Figure 4.** X-band EPR spectra (black lines) of [(Tp$^{Ph,Me}$)Co(**L$_{O,O}$**)] and [(Tp$^{Ph,Me}$)Co(**L$_{O,S}$**)] complexes and corresponding simulations (gray lines).

**Table 2.** Bond Lengths and $\tau$ Values for [(Tp$^{Ph,Me}$)M(**L**)] Complexes[a]

| ligand (L) | M−N bond length (Å)[b,d] | M−O bond length for anionic donor atom (Å)[d] | M−X bond length for neutral donor atom (Å, X = O,S)[d] | $\tau$ value[d] |
|---|---|---|---|---|
| maltol | 2.11, 2.10 | 1.94, 1.95 | 2.18, 2.08(O) | 0.69, 0.37 |
| thiomaltol | 2.12, 2.11 | 2.06, 1.98 | 2.34, 2.37 (S) | 0.66, 0.24 |
| 3,4-HOPO | 2.13, 2.12 | 1.97, 1.96 | 2.05, 2.02 (O) | 0.44, 0.43 |
| 3,4-HOPTO | 2.22, 2.13 | 2.07, 1.96 | 2.29, 2.37 (S) | 0.60, 0.20[c] |
| 1,2-HOPO | 2.11, 2.19 | 1.97, 2.05 | 2.09, 2.10 (O) | 0.64, 0.28 |
| 1,2-HOPTO | 2.16, 2.12 | 2.08, 1.97 | 2.32, 2.34 (S) | 0.54, 0.17 |

[a] M = $Zn^{2+}$ (left); M = $Co^{2+}$ (right). [b] Average of three bonds from Tp$^{Ph,Me}$ ligand. [c] Average of four $\tau$ values found in asymmetric unit; individual values are 0.04, 0.10, 0.26, and 0.38. [d] Values for zinc(II) complexes taken from refs 16 and 22.

**Table 3.** EPR Simulation Parameters for [(Tp$^{Ph,Me}$)Co(**L**)] Complexes

| ligand (L) | $g_x$ | $g_y$ | $g_z$ | $D$ (cm$^{-1}$) | $E/D$ | $A_z$ ($^{59}$Co) $10^{-4}$ cm$^{-1}$ |
|---|---|---|---|---|---|---|
| maltol | 2.60 | 2.56 | 2.32 | −8 | 0.210 | 110 |
| thiomaltol | 2.60 | 2.52 | 2.26 | −3 | 0.190 | 106 |
| 3,4-HOPO | 2.70 | 2.40 | 2.20 | −3 | 0.152 | 120 |
| 3,4-HOPTO | 2.80 | 2.40 | 2.20 | −3 | 0.180 | 142 |
| 1,2-HOPO | 2.58 | 2.40 | 2.20 | −12 | 0.152 | 112 |
| 1,2-HOPTO | 2.62 | 2.40 | 2.20 | −11 | 0.180 | 115 |

the upper $\pm^1/_2$ doublet. The relative contributions of these two sets of transitions to the observed spectrum are then determined by size of the axial zfs, $D$, which is required to be negative, on the basis of the temperature-dependence of the NMR spectra (all of the chemical shifts increase with decreasing temperature, discussed below). Rhombicity in the zfs ($E/D$) shifts the high-field derivative ($\pm^3/_2$) to lower field and increases the intensity of the derivative feature at $g = 4$ ($\pm^1/_2$, compare, for example, 3,4-HOPO and 3,4-HOPTO). For each pair of hydroxypyridinone ligands (HOPO and HOPTO), substitution of a neutral carbonyl oxygen donor with a neutral thionyl sulfur appears to shift the high-field derivative to lower field and broaden it significantly and a greater influence of the features ascribed to the upper $\pm^1/_2$ doublet, implying increased $E/D$. This is to be expected on changing the coordination sphere from $N_3O_2$ to $N_3OS$. The opposite appears true for maltol and thiomaltol, where both $D$ and $E/D$ *decrease* with the sulfur substitution.

The appearance of individual spectra is extremely sensitive to temperature and power (Figure S1), indicating either rapid passage effects or mixing of the two doublets. This is not inconsistent with previous studies of cobalt-substituted metalloproteins. Identification of the ground doublet has often been achieved by following the temperature-dependence of the signal strength.[53−60] Of those that provide simulations, the spectra are usually interpreted as arising from an effective $S = {}^1/_2$ system, leaving the identity of the ground doublet unassigned.[28,61−66] The data we present in Figure S1 clearly show that, even by 5 K, the features ascribed to the $\pm^3/_2$ doublet are disappearing, while those from the $\pm^1/_2$ doublet persist to much higher temperatures. Therefore, data collection at slightly elevated temperatures fully justifies interpretation as an effective $S = {}^1/_2$ ground state. A more recent MCD study[67] of a five-coordinate Co in methionyl aminopeptidase has suggested that, in idealized five-coordinate geometries ($D_{3h}$ or $C_{4v}$), the zfs is expected to be small and that the observed MCD intensity can arise simultaneously from the $^3/_2$ and $^1/_2$ levels. This is fully consistent with our interpretation of the current EPR data.

Compared to the frozen-solution EPR spectra, fluid solution NMR spectra of the cobalt compounds are remarkably simple (Figure 5). Peak assignments are summarized in Table 4. Each complex shows only five resonances attributable to the Tp$^{Ph,Me}$ ligand. This observation has two implications; the first is that the phenyl rings have sufficiently free rotation that the ortho and meta phenyl protons are magnetically similar enough to collapse into a single, unresolved line. Integration of the room-temperature spectrum for [(Tp$^{Ph,Me}$)Co(maltolato)], for example, gives a 12-proton intensity for the resonance at −50 ppm. The para phenyl protons are minimally affected, showing negative paramagnetic shifts of <10 ppm.

The second, perhaps more important implication of the simplicity of the NMR spectra is the apparent equivalence of the three pyrazolate rings. The large, negative chemical

(53) Werth, M. T.; Tang, S. F.; Formicka, G.; Zeppezauer, M.; Johnson, M. K. *Inorg. Chem.* **1995**, *34*, 218−228.
(54) Scarpellini, M.; Wu, A. J.; Kampf, J. W.; Pecoraro, V. L. *Inorg. Chem.* **2005**, *44*, 5001−5010.
(55) Adrait, A.; Jacquamet, L.; Le Pape, L.; de Peredo, A. G.; Aberdam, D.; Hazemann, J. L.; Latour, J. M.; Michaud-Soret, I. *Biochemistry* **1999**, *38*, 6248−6260.
(56) Jimenez, H. R.; Salgado, J.; Moratal, J. M.; MorgensternBadarau, I. *Inorg. Chem.* **1996**, *35*, 2737−2741.
(57) Kuo, L. C.; Makinen, M. W. *J. Am. Chem. Soc.* **1985**, *107*, 5255−5261.
(58) Dickinson, L. C.; Chien, J. C. W. *J. Am. Chem. Soc.* **1983**, *105*, 6481−6487.
(59) Makinen, M. W.; Maret, W.; Yim, M. B. *Proc. Natl. Acad. Sci. U.S.A.* **1983**, *80*, 2584−2588.
(60) Kardinahl, S.; Anemüller, S.; Schäfer, G. *Biol. Chem.* **2000**, *381*, 1089−1101.
(61) Tubbs, K. J.; Szajna, E.; Bennett, B.; Halfen, J. A.; Watkins, R. W.; Arif, A. M.; Berreau, L. M. *Dalton Trans.* **2004**, 2398−2399.
(62) Shapir, N.; Osborne, J. P.; Johnson, G.; Sadowsky, M. J.; Wackett, L. P. *J. Bacteriology* **2002**, *184*, 5376−5384.
(63) Doi, Y.; Lee, B. R.; Ikeguchi, M.; Ohoba, Y.; Ikoma, T.; Tero-Kubota, S.; Yamauchi, S.; Takahashi, K.; Ichishima, E. *Biosci. Biotech. Biochem.* **2003**, *67*, 264−270.
(64) Crowder, M. W.; Yang, K. W.; Carenbauer, A. L.; Periyannan, G.; Seifert, M. E.; Rude, N. E.; Walsh, T. R. *J. Biol. Inorg. Chem.* **2001**, *6*, 91−99.
(65) Bennett, B.; Holz, R. C. *Biochemistry* **1997**, *36*, 9837−9846.
(66) Bienvenue, D. L.; Bennett, B.; Holz, R. C. *J. Inorg. Biochem.* **2000**, *78*, 43−54.
(67) Larrabee, J. A.; Leung, C. H.; Moore, R. L.; Thamrong-nawasawat, T.; Wessler, B. S. H. *J. Am. Chem. Soc.* **2004**, *126*, 12316−12324.

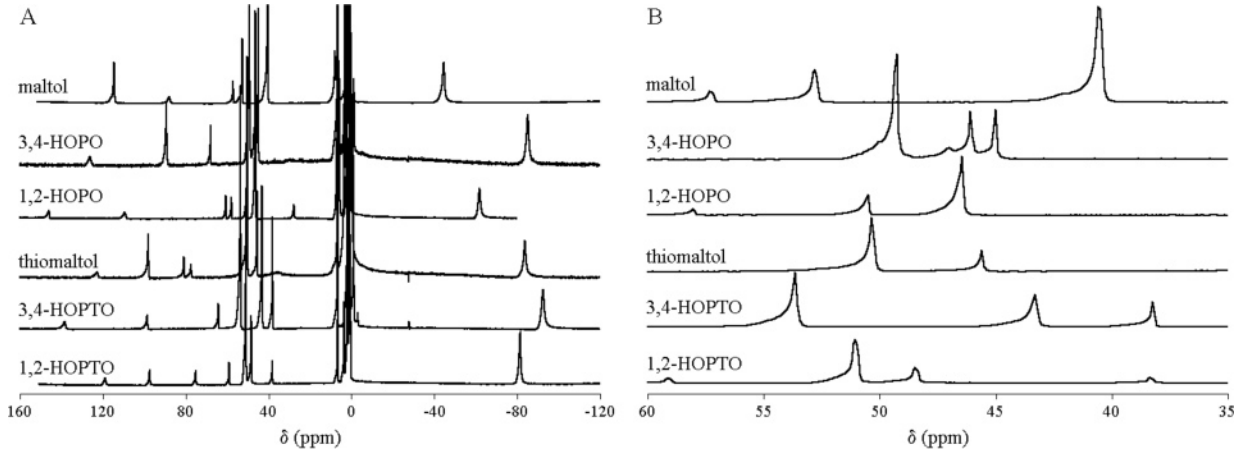


**Figure 5.** (A) 300 MHz $^1$H NMR spectra of [(Tp$^{Ph,Me}$)Co(**L$_{O,O}$**)] and [(Tp$^{Ph,Me}$)Co(**L$_{O,S}$**)] complexes. (B) Expansion of the congested region between 35 and 60 ppm. Parts A and B are plotted on different vertical scales for clarity.

**Table 4.** Room-Temperature NMR Assignments for [(Tp$^{Ph,Me}$)Co(**L**)] Complexes

| | Tp$^{Ph,Me}$ ligand | | | | | ancillary ligand | | | |
|---|---|---|---|---|---|---|---|---|---|
| ligand (L) | 3Ph (*o*, *m*) | 3Ph (*p*) | 4H | 5Me | BH | | | | |
| maltol | −44 | −1 | 53 | 41 | 88 | | 42 (6H) | 57 (5H) | 115 (2CH$_3$) |
| 3,4-HOPO | −85 | −1 | 45 | 49 | 126 | 46 (NCH$_3$) | 47 (6H) | 68 (5H) | 90 (2CH$_3$) |
| 1,2-HOPO | −62 | 0.5 | 47 | 51 | 146 | 28 (3H) | 58 (4H) | 61 (5H) | 110 (6H) |
| thiomaltol | −84 | −0.3 | 46 | 50 | 123 | | 77 (6H) | 81 (5H) | 99 (2CH$_3$) |
| 3,4-HOPTO | −92 | −1 | 43 | 54 | 134 | 43 (NCH$_3$) | 43 (2CH$_3$) | 63 (6H) | 95 (5H) |
| 1,2-HOPTO | −81 | 0.5 | 48 | 51 | 119 | 39 (5H) | 60 (4H) | 75 (6H) | 98 (3H) |

shift of the ortho/meta protons is common for substituents in the pyrazole 3-position in [Co(Tp$^x$)$_2$] complexes.[68] It implies that the *g*-tensor, in fluid solution, is roughly oriented through the 3-fold axis defined by the Tp ligand. This requires that all three pyrazole donors of the Tp$^{Ph,Me}$ ligand be chemically equivalent. Considering a square-pyramidal arrangement about cobalt(II) and the tripodal arrangement of the pyrazole donors in the Tp$^{Ph,Me}$ ligand, the only possible arrangement is the one observed in the crystal structures (Figure 2), where two pyrazole donors are in the equatorial plane and the third is in the axial position. Therefore, the observed symmetry must be due to a change in coordination geometry and/or dynamic process in solution. The symmetry equivalence of the pyrazole 3-, 4-, and 5-substituents requires that there be a process to interconvert the three pyrazolate rings. This indicates the presence of some fluxional behavior, such as dissociation/recombination or a Berry pseudorotation, as mentioned above.

To explore this possibility further, we examined the NMR temperature-dependence of all six complexes (Figure S2). No fluxional processes are frozen out within the accessible temperature range (237−307 K). The absence of any points of coalescence leaves open the possibility that a dissociation/recombination process is operable to temperatures below 237 K, but this would require an extremely low barrier and therefore very weak binding of the neutral donor atom. For this reason, we favor the presence of a pseudorotation mechanism.

The ancillary ligands display one well-resolved resonance for each type of proton. This implies that any process that interconverts structures must retain the magnetic inequivalence of the protons on the ancillary ligand. Thus, it appears that the best description of these complexes in solution is a time-averaged structure of $C_s$ symmetry, with the *z* axis passing through the apical boron of Tp$^{Ph,Me}$ and bisecting the two Co−O/S bonds of the ancillary ligand, and the symmetry plane defined by the plane of the ancillary ligand. This description is further supported by the ancillary ligand chemical shift pattern, with all positive shifts, suggesting none occupy a position >54.7° off the *z* axis of the Co(II) ion. This is also consistent with the ligand-field region of the optical spectra, as $C_s$ symmetry orders the d-orbital manifold ($x^2 - y^2$, $z^2$ and $xy$ = A′; $xz$ and $yz$ = A″) such that a subset of the ligand field transitions are forbidden, leading to only weak intensity. The actual mechanism of this interconversion, as well as its presence or absence in the analogous Zn complexes, is the subject of an ongoing investigation.

## Conclusions

The role of MMPs in a variety of human diseases is well recognized. In the process of developing bioinorganic approaches to inhibiting these zinc-containing hydrolytic enzymes, the need for a spectroscopic handle on the MMP active site is apparent. Several tris(pyrazolyl)borate model complexes with cobalt(II) have been prepared and studied by structural and spectroscopic methods. The compounds presented here indicate that chelating bidentate ligands generally replicate the zinc(II) coordination geometry well but with a greater tendency toward square pyramidal geometries due to ligand-field stabilization effects. EPR spectra of the cobalt complexes are consistent with a pentacoordinate metal ion and are similar in appearance to other cobalt-substituted metalloenzymes. The NMR spectra

(68) Jesson, J. P. *J. Chem. Phys.* **1967**, *47*, 582−591.

indicate that the asymmetry is averaged in solution, with dynamic motion interchanging the three chelating pyrazolates at a rate faster than the NMR time scale, even at 237 K. We anticipate that the cobalt(II)-containing model complexes presented here may be a useful tool for probing the active site of inhibited MMPs.

**Acknowledgment.** We thank Prof. Arnold L. Rheingold and Dr. Lev N. Zakharov (U.C. San Diego) for help with the X-ray structure determinations, and Prof. Emmanuel A. Theodorakis and Prof. Cliff Kubiak (U.C. San Diego) for use of the FT-IR. F.E.J. has been supported in part by a GAANN fellowship (GM-602020-03). This work was supported by the University of California, San Diego, a Chris and Warren Hellman Faculty Scholar award to S.M.C., the American Heart Association (0430009N to S.M.C.) and the National Science Foundation (CHE-0518189 and CHE-0216277 (MRI) to D.L.T.). S.M.C. is a Cottrell Scholar of the Research Corporation.

**Supporting Information Available:** Two figures, showing temperature- and power-dependent EPR of [$Tp^{Ph,Me}$Co(1,2-HOPO)] (Figure S1) and temperature-dependent NMR of [$Tp^{Ph,Me}$Co(1,2-HOPTO)] (Figure S2) are included and X-ray crystallographic data in CIF format. This material is available free of charge via the Internet at http://pubs.acs.org.

IC060901U